Computational Study of the Structural and Electronic Properties of Dopant Ions in Microporous AlPOs. 2. Redox Catalytic Activity of Trivalent Transition Metal Ions

Iman Saadoune,* Furio Corà, Maria Alfredsson, and C. Richard A. Catlow

Davy Faraday Research Laboratory, The Royal Institution of Great Britain 21 Albermarle St., London W1S 4BS, U.K.

Received: October 23, 2002

Periodic ab initio QM calculations are employed in order to study the structure and redox properties of Cr, Mn, Fe, and Co trivalent transition metal dopants in AlPO-34. Our results show that the local environment of Mn and Co dopants is a distorted tetrahedron due to Jahn−Teller distortions. The bonding between the Me^{III} dopants and the neighboring oxygens is ionic in nature; and explains the Lewis acidity of the Me^{III} ions. The replacement energy ΔE_{III} of the 3+ dopant ions in AlPO-34 increases linearly as a function of the Me−O bond distance. Finally, the calculated redox energies of the Me^{II}/Me^{III} couples indicate that, among the transition metal ions investigated, Fe is the most stable in the 3+ oxidation state, whereas Mn is the most stable as 2+ ion. Cr and Co, instead, have intermediate behavior and can switch more easily between the two oxidation states. These results contribute to elucidate the mechanistic details of catalytic processes occurring in MeAlPOs.

1. Introduction

Microporous aluminophosphates (AlPOs), when activated via the inclusion of dopant ions in the framework, have widespread applications in the field of heterogeneous catalysis.[1,2] Both acid and redox activity can be conferred to the materials via an appropriate choice of the dopant. Brønsted acidity, for instance, is linked with the presence of low valence metal ions in the framework, such as Mg^{2+} or Ni^{2+} replacing for Al^{3+} or Si^{4+} replacing for P^{5+}, that require the presence of the acid protons for charge compensation. Redox activity is instead achieved with transition metal dopants such as Cr, Mn, Fe, or Co that can reversibly change their oxidation state in the AlPO framework. AlPO materials doped with transition metal ions (MeAlPOs) have been shown to catalyze with high selectivity the oxidation of hydrocarbons.[3,4]

We have undertaken an extensive quantum mechanical study on several 2+ and 3+ dopant ions, to understand the properties associated with the presence of heteroatoms in AlPO frameworks. In a previous paper,[5] we reported results on the structure, electronic, and acid properties of divalent ions; in this paper, we concentrate instead on tri-valent transition metal ions and their redox properties.

Several transition-metal-substituted aluminophosphate molecular sieves show activity for selective oxidation of hydrocarbons, a reaction of immense importance in the chemical industry.[3] For example, the conversion of cyclohexane into cyclohexanone is the center-piece for the commercial production of nylon,[4] whereas the partial oxidation of the terminal methyl groups in alkanes is of considerable interest as potential feedstock for the fine chemicals and pharmaceutical industries. One of the advantages of MeAlPOs over other heterogeneous catalysts in selective oxidation reactions is their ability to employ molecular oxygen as oxidant,[6] reducing the cost of sacrificial oxidants and polluting byproducts.

Despite the economic importance of selective oxidation reactions, developing appropriate catalysts that compromise between redox activity and selectivity remains a challenging scientific task.[7]

To understand the redox activity of doped AlPOs, we have investigated the chemistry that follows doping of the AlPO-34 framework with redox-active trivalent transition metal ions, namely, Mn^{III}, Fe^{III}, Co^{III}, and Cr^{III}. This study is complemented by the characterization of other trivalent substitutional ions, namely B^{3+} and Ga^{3+}, to understand the energetics of the Me^{3+}/Al^{3+} framework substitutions. The results of our calculations are employed to examine the mechanistic details of selective oxidation reactions catalyzed by MeAlPOs available in the literature.[6,8]

2. Computational Details

The doped framework of AlPO-34, chosen as a representative of the class of microporous AlPOs, is described in our calculations with a supercell model, using periodic boundary conditions. The level of doping used in our calculations is of one dopant ion per unit cell of the host AlPO34 framework, composed of 36 ions. The calculations are performed at the Hartree−Fock (HF) level of theory, as implemented in the latest version of the program CRYSTAL.[9] The electronic distribution of the system is described as a linear combination of atomic orbitals, and the basis functions are expressed analytically as a contraction of Gaussian-type orbitals. The basis sets employed to describe the host AlPO framework and the transition metal dopants are the same as in ref 5. For Ga and B metal ions, we used 86-4111d4G (derived for GaAs and GaN structures), and 6-21d1G basis sets (derived for BN and BP), respectively. All of the basis sets are available from the online library of the CRYSTAL code.[10] We used the HF Hamiltonian in our work because it includes the exact expression for exchange forces, which is expected to be important for the description of the spin state of open-shell transition metal ions. The HF calculations on the undoped framework[11] yielded an equilibrium structure in very close agreement with the experiment; we expect, therefore, the results of HF calculations on the doped systems to provide us with a reliable description of the local

* To whom correspondence should be addressed. E-mail: iman@ri.ac.uk.

10.1021/jp027286+ CCC: $25.00
Published on Web 03/12/2003

environment of the metal ions that can be usefully compared with experimental data, for instance, from X-ray absorption spectroscopy.[12,13]

Further details about the computational settings applied in our periodic QM calculations are reported in ref 5.

From the results of the QM periodic calculations, we can obtain direct quantitative information about the electronic properties and the local structural environment of metal dopants in AlPOs and an accurate characterization of the long-range structure of the host AlPO framework. The calculated energy of the pure and doped frameworks can also be combined to calculate the substitution energy of the dopant in the AlPO framework. Because the synthesis of MeAlPOs is performed in an aqueous medium, by hydrothermal synthesis,[14,15] we have considered as suitable states for the +3 ions outside the framework their hexa-aqua complexes, $[Me(H_2O)_6]^{3+}$. Of course, this represents an approximation, as only the first solvation sphere of the 3+ ions is included; nonetheless, it represents a suitably simple computational model of the solvated ions. The replacement energy of the 3+ dopant ions for a framework Al^{3+} species are calculated according to the following expression:

$$[Me(H_2O)_6]^{3+} + \text{ALPO-34} \xrightarrow{\Delta E_{III}} Me^{III}\text{AlPO-34} + [Al(H_2O)_6]^{3+} \quad (1)$$

$$\Delta E_{III} = E(Me^{III}\text{AlPO-34}) + E[Al(H_2O)_6]^{3+} - E[Me(H_2O)_6]^{3+} - E(\text{ALPO-34}) \quad (2)$$

where ΔE_{III} indicates the ease of inclusion of the Me^{3+} in AlPO framework.

To obtain the replacement energies ΔE_{III} for the metal dopants according to eq 2, we have calculated in a consistent way the energies corresponding to the molecular species, i.e., the hexa-aqua complexes, $[Me(H_2O)_6]^{3+}$and $[Al(H_2O)_6]^{3+}$, and the energies of the perfect and defective solids, AlPO-34 and MeAlPO-34. In particular we have employed the same basis set for the Al^{3+} and Me^{3+} ions in molecular and solid-state calculations. The water molecules are described with a standard 6-31G* basis set.[16] Improvement of the basis set to 6-311+G**[17] for the hexahydrated ions causes changes of less than 0.0008 Å in the equilibrium Me−O bond distances and less than 0.16 eV in the calculated values of ΔE_{III} (eq 2).

In this section, we shall examine the results concerning the solvated ions (molecular species), whereas the doped framework structures (solid-state systems) are discussed in section 3.

2.1. Molecular Calculations. The geometries of all of the molecular systems have been optimized at the HF level of theory using the Gaussian 98[18] and CRYSTAL[9] programs. No symmetry constraints were imposed on any of the molecules investigated. In the optimized structure, the hexa-aqua complexes of Al^{3+}, Ga^{3+}, Fe^{3+}, and Cr^{3+} are stable in an octahedral symmetry with point group T_h. The optimized structures of $[Mn(H_2O)_6]^{3+}$ and $[Co(H_2O)_6]^{3+}$, instead, have a lower symmetry configuration (point group D_{2h}) due to Jahn−Teller distortions. For the complexes of open-shell transition metal ions, we have optimized all possible spin states, compatible with the number of d electrons. All of the geometry optimizations of the $[Me(H_2O)_6]^{3+}$ complexes have been followed by frequency calculations, to ensure that the structures obtained are true minima on the potential energy surface. No imaginary frequencies are present. Our calculations found that all of the transition metal ions studied in this work are stable in the high spin state.

TABLE 1: Calculated and Experimental Me−O Distances for Hexahydrated Molecular Ions $[Me(H_2O)_6]^{3+}$[a]

	R (Me−O)/Å		
Me	this work	other theoretical works	exp
Al^{3+}	1.918	1.935[19]	1.900[22]
Ga^{3+}	1.988	1.998[20]	1.954[23]
Cr^{3+}	2.032	2.025[21]	1.960[25]
Mn^{3+}	2.063	2.042[21]	1.991[24]
Fe^{3+}	2.060	2.052[21]	2.010[25]
$Co^{3+}{}_l$	1.928	1.933[21]	1.873[24]
$Co^{3+}{}_h$	2.020		

[a] For Co^{3+}, the symbols "l" and "h" indicate low and high spin states, respectively.

We attribute these results to the relatively low ligand field splitting of the Me-*d* levels caused by the water ligands.

The results of our calculations are compared with previous computational[19−21] and experimental studies[22−25] in Table 1. Although there is good agreement with the previous computational studies, the comparison with experimental results[22−25] (Table 1) is less satisfactory and indicates the inadequacy of our gas-phase-like $[Me(H_2O)_6]^{3+}$ complexes in representing Me^{3+} ions either solvated or in a crystalline matrix. For Co^{3+} and Mn^{3+}, which are both disproportionate in aqueous solutions, we compare the calculated Me−O distances with X-ray diffraction data obtained from of an isomorphous crystal structure of cesium alum salts $[CsMe^{III}(SO_4)_2 \cdot 12\ H_2O]$, in which Co^{3+} and Mn^{3+} are found as a hexa-hydrated unit, with an almost regular octahedral coordination.[24] The experimental values of the Me−O bond distances are shorter than the calculated ones by as much as 0.07 Å, which is far greater than expected from the quality of the calculations performed. This large difference is due to the long-range effects present in the aqueous solutions and the crystalline matrix but not in the isolated hexa-aqua complexes. Both in the water solutions and in the alum salts, the strong hydrogen-bonds which link the first to the second hydration sphere polarize the water molecules and shorten the Me-O bonds.[26] Moreover, the steric pressure exerted on the $[Me(H_2O)_6]^{3+}$ core from the crystalline matrix, shortens the Me−O bond distance with respect to the isolated complex. We can, however, assume that these "long-range" forces affect systematically ions with the same charge (i.e., all of the Me^{3+} ions examined here), and the error introduced will cancel out when considering energy differences, such as those of eq 2 needed to calculate ΔE_{III}.

On the basis of assumptions from the experimental work on Alum Salts, Akesson et al.[21] assumed in their work that Co^{3+} in the hexa-aqua complex is stable in the low spin state, $t^6{}_{2g}\ e^0{}_g$; we have instead investigated both the low and high spin states for Co^{3+} and found the high spin state $t^4{}_{2g}\ e^2{}_g$ to be more stable. In Table 1, we report the calculated Co−O bond distances for both spin states, and we find that the difference in the Me−O distance between the two spin states is correlated with their ionic radius: the Co^{3+} in high spin is larger than Co^{3+} in low spin. This result agrees with previous work.[27]

3. Results

We shall now present the results of our calculations on the doped AlPO-34 framework, considering separately the structural details, electronic properties, energetics, and redox properties of the different MeAlPO-34 materials investigated.

3.1. Local Environment of the Trivalent Metal Dopants. The structural parameters that describe the local environment of the Me^{III} dopants in AlPO's, obtained from our QM structural

TABLE 2: Calculated Me−O Bond Distances (in Å) for Trivalent Metal Centers in MeAlPO-34 Catalysts[a]

Me	R(Me−O_1)	R(Me−O_2)	R(Me−O_3)	R(Me−O_4)	⟨*R*⟩	Exp
B	1.46	1.48	1.53	1.55	1.50	
Ga	1.80	1.81	1.81	1.82	1.81	1.82[32]
Cr	1.88	1.88	1.89	1.91	1.89	
Mn	1.86	1.87	1.91	1.91	1.88	1.85[28]
Fe	1.86	1.86	1.87	1.88	1.86	1.86[29]
Co	1.83	1.84	1.85	1.86	1.84	1.89[30]
Al	1.72	1.72	1.73	1.73	1.73	1.73[31]

[a] Experimental EXAFS or crystallographic data, where available, are also reported.

TABLE 3: Calculated Value of the T−O−P Angles (in degrees) in the MeAlPO-34 Frameworks[a]

Me	Me−O−P	T−O−P	Al−O−P
B	151.34	150.13	149.89
Cr	144.95	147.99	148.60
Mn	138.74	147.54	149.30
Fe	144.58	148.72	149.55
Co	141.44	147.53	148.75
Ga	144.90	148.99	149.81
Al	148.59	148.59	148.59

[a] Me−O−P is the average of the four angles on the oxygens that are nearest neighbor to the dopant, whereas the column T−O−P indicates the value of the angle averaged over the whole structure. The column indicated as Al−O−P refers to the angle around all oxygen ions in the structure that are not nearest neighbors of the dopant.

optimization and from experimental data where available, are summarized in Tables 2 and 3. These include the four Me−O bond distances, R(Me−O_n), between the Me dopant and its four nearest neighbor oxygens; the average Me−O bond distance, ⟨*R*⟩; and the average Me−O−P angle around the four oxygens, that are nearest neighbors of Me. We also report the value of the T−O−P angle (T = Me and Al), averaged over all of the oxygen ions of the structure.

The calculated Me−O bond lengths reported in Table 2 agree well with the experimental values obtained by EXAFS measurements on MeAlPOs,[28,29,30] as well as with the crystallographic structure of berlinite[31] and quartz-structured GaPO.[32] With the exception of the small B^{3+} ion, all of the other Me−O bonds examined are considerably longer than the Al−O of the host framework. The inclusion of the dopants in the framework will therefore induce a structural strain in the surrounding region.

We further note in Table 2 that the tetrahedral coordination environment of Ga^{3+} and Fe^{3+} ions shows only minor differences (less than 0.02 Å) in the four Me−O bond lengths, whereas for Cr, Co, and especially Mn, the coordination is much more distorted. Even bigger distortions were found in the study of Me^{2+} dopant ions in AlPO-34 and of Me^{3+} ions in chabasite.[33] The latter two frameworks are charge-compensated by an acidic proton on one oxygen nearest neighbor of the dopant, and the distortion is due mostly to the chemical inequivalence of the oxygens. The protonated oxygen, in fact, behaves differently from the three nonprotonated ones and has a much longer (by ∼0.15 Å) bond distance to both its nearest Me and P ions. The situation is different for the Me^{3+} dopant ions in AlPO-34; no charge compensation is required in this case, and all of the nearest neighbor oxygens of the metal dopant are chemically equivalent. The distortion in the local coordination environment of the Me^{3+} dopants is instead due mainly to Jahn−Teller effects. Although closed-shell dopants with a formal charge of +2, such as Mg, Ca, and Sr, are in a local distorted environment, closed-shell +3 ions occupy instead a much more regular crystalline position. The only exception to this rule is B^{3+}, which is too small to retain the undistorted tetrahedral coordination of Al sites in the AlPO. In ref 33, we found that B^{3+} in the silica framework of Chabasite is stable in a trigonal coordination, in which the B−OH bond is effectively broken; the local environment is not the same for B^{3+} in AlPO-34, where the coordination of B^{3+} is still tetrahedral; the small ionic size of B^{3+}, however, causes a significant distortion of the individual B−O bond distances.

Although our calculated bond distances for Al, Ga, Fe, and Mn ions are in good agreement with the experimental values, the calculated bond distance for Co is underestimated by 0.05 Å. Our calculations correspond to a fully oxidized form of the CoAlPO framework, in which only Co^{III} ions are present. The underestimation of the calculated Co−O bond distance, compared to the experimental one, suggests that in the experimental CoAlPO sample some of the Co ions are reduced and that a mixture of Co^{II} and Co^{III} is present in the framework. Because the XAS data are element-specific, but cannot differentiate its oxidation state,[34] the experimental results represent an average of the properties of all of the Me dopants present in the solid. A fraction of Co ions in 2+ oxidation state will cause the increase of the Me−O bond distances observed experimentally. The redox potential of the Co^{II}/Co^{III} couple in AlPO-34 discussed in section 3.4 confirms the stability of Co as 2+ ion in the AlPO framework and is consistent with the ease of reduction of Co^{3+}.

Let us now consider the changes that occur in the T−O−P framework angles in the doped MeAlPO frameworks. We have shown in ref 5 that this information provides us with a quantitative estimate of the extent of structural distortion around the metal dopant. We see in Table 3 that the average value of the calculated Me−O−P angle, for the four nearest neighbor oxygens of the metal dopant, is lower than the original Al−O−P angle in the pure AlPO framework. The largest difference, of ∼10°, is shown by the Mn^{III} dopant, which is also the ion whose environment is most distorted (with the exception of B^{3+}). The oxygens next to the Mn dopant are therefore the framework atoms that sustain the largest structural strain upon doping of the framework. The Me−O−P angles in Co-, Fe-, and Cr-doped materials are instead less distorted. Moving away from the dopant, the angles appear to be only marginally affected, and the value of the Al−O−P angles in the defective AlPO, averaged over the whole structure, remains close to the value of the Al−O−P angle in the undoped AlPO framework. We conclude therefore that the Me^{III} dopants examined here cause only a short-ranged structural stain, which is appreciable only around the metal dopant itself.

3.2. Electronic Properties of the Dopants. Let us now investigate the properties of the bonding between the Me^{3+} dopants and the neighboring oxygens in the framework. Results of a Mulliken population analysis of the electronic distribution are reported in Table 4. The high net charge of the Me^{3+} dopants and the low overlap population q_b(Me−O) between dopant and neighboring oxygens suggests that the bonding of the Me^{3+} dopant to the host framework is ionic in nature, as with the host Al^{3+}, which was found to be ionic in our previous work.[11] Again, the behavior of B^{3+} differs, with a lower net ionic charge and a higher overlap population, suggesting that B^{3+} bonds covalently to the neighboring oxygens. This result is not surprising as B^{3+} is a very small ion and is more electronegative compared to Al^{3+} and the other dopants.

To support our findings, we show the difference electron density maps (obtained as the difference between the electron density in the solid and the superposition of isolated formal ions) for the Me−O bond in the B-, Ga-, and Fe-doped AlPO

TABLE 4: Mulliken Population Analysis of the Electronic Distribution of Me^{III} Substitutional Ions in AlPO-34[a]

Me	*Q*(O)	*Q*(Me)	q_b(Me−O)
B	−1.13	1.57	0.22
Cr	−1.24	2.15	0.08
Mn	−1.24	2.17	0.09
Fe	−1.26	2.23	0.10
Co	−1.26	2.20	0.10
Ga	−1.29	2.33	0.11
Al	−1.26	2.20	0.14

[a] The symbol *Q* refers to the net ionic charges on the metal dopant [*Q*(Me)] and the average of its four nearest neighbor oxygens [*Q*(O)]; q_b denotes the Me−O bond population, in |e|, averaged over the four nearest neighbors.

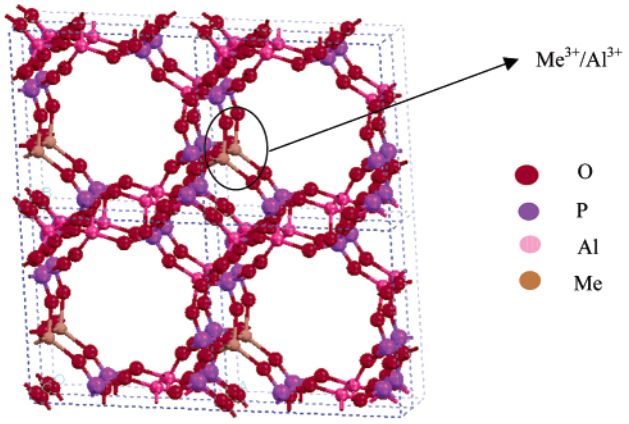

Figure 1. Representation of a Me^{III} substitutional ion in the AlPO-34 framework, described with a supercell model.

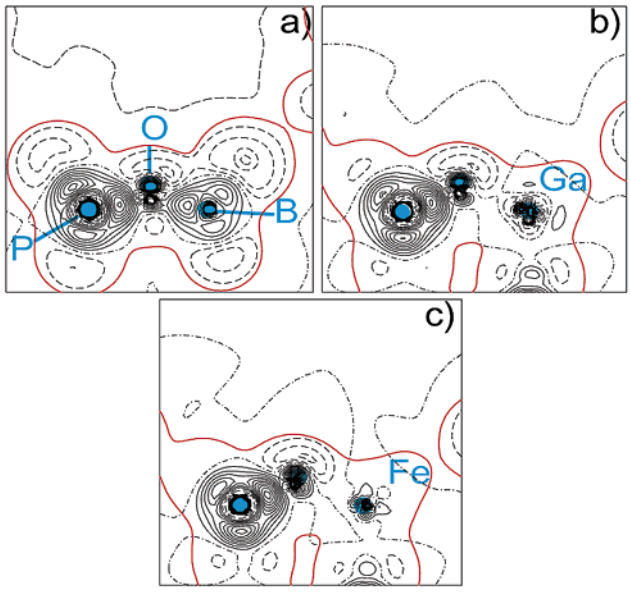

Figure 2. Difference electron density maps (solid minus isolated formal ions), plotted in a plane containing one B−O−P (a), Ga−O−P (b), or Fe−O−P (c) unit in AlPO-34. Continuous and dashed lines correspond to positive and negative densities, plotted between − 0.1 and 0.1 au (|e| $bohr^{-3}$) at linear steps of 0.01 au. The red line is the total electron density level of 0.01 au and indicates the framework size.

frameworks (Figure 2). The maps are drawn in a plane which contains the metal dopant, one of its oxygen neighbors, and the phosphorus ion bonded to the latter oxygen. From the difference density plots, we clearly see an appreciable electronic redistribution in the covalent P−O bonds, whereas only minor features are present around the Ga and Fe dopants, which is consistent with an ionic description of the dopants in the AlPO framework. The other Me ions behave similarly to Ga and Fe. This result is in agreement with the Lewis acid behavior displayed by the MeAlPO materials.[29,35−38] For the B^{3+}-doped AlPO, instead, there is a significant electronic redistribution around B, which enforces our initial suggestion that the bonding of B^{3+} in the AlPO framework is of covalent nature.

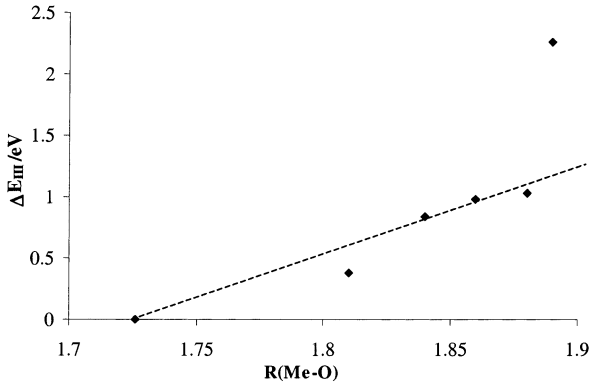

Figure 3. Calculated replacement energy ΔE_{III} for the dopant ions examined (in eV), as a function of the average metal−oxygen bond distance, in Å.

TABLE 5: Calculated Replacement Energy ΔE_{III} (in eV) of a Framework Al with Me^{III} Dopants, According to Eq 2

Me	Ga	Cr	Co	Mn	Fe
ΔE_{III}	0.377	2.258	0.844	1.034	0.980

The transition metal ions investigated have a partially filled d shell, with an electronic configuration ranging between the $d^{(3)}$ of Cr^{3+} to the $d^{(6)}$ of Co^{3+}. When they are isomorphously substituted for Al in the AlPO-34 framework, our calculations show that all of the transition metals investigated are stable in the spin state with the highest multiplicity compatible with their count of d electrons. The high spin state would be expected, owing to the low crystal field splitting caused by the tetrahedral coordination of the transition metal ions. The partially covalent character of the oxygen ligands with the phosphorus ions, discussed earlier, decreases their net charge and makes the crystal field they create insufficient to stabilize low spin states on the transition metals. A higher crystal (or ligand) field splitting is required to stabilize a pairing of the d electrons; this is achieved, for example, in ionic oxides where the open shell transition metal ions are in an octahedral environment, such as the $LaMO_3$ perovskites. Calculations performed with the same Hamiltonian, basis set for the transition metal ion, and computational settings as used here indicate that in the perovskite environment the d^6 Co^{3+} ions is stable in the low spin state $t_{2g}^6 e_g^0$, whereas the high ($t_{2g}^4 e_g^2$) spin state is unstable by 0.93 eV.[39] The latter result is in agreement with the experimental evidence on $LaCoO_3$.

3.3. Substitutional Energy of a Framework Al with Me^{3+} Dopants. The calculated replacement energies ΔE_{III} of a framework Al with different Me^{3+} dopants, according to reaction 1, are summarized in Table 5. The small B^{3+} ion is not included, because of its instability in coordination number 6, which makes the hexa aqua complex $[B(H_2O)_6]^{3+}$ inappropriate to describe an hydrated B^{3+} ion.

When examining the variation of the replacement energies with the average Me−O bond distance (see Figure 3), we find that, with the exception of Cr^{III}, ΔE_{III} increases linearly as a function of the Me−O bond distance. As for the 2+ dopant ions examined in ref 5, our results show that the larger the size of the dopant, the greater its substitution energy in the AlPO framework.

TABLE 6: Redox Energies ΔE (in eV) for the Transition Metal Ions Examined in AlPO-34

Me^{III}/Me^{II}	Cr^{III}/Cr^{II}	Mn^{III}/Mn^{II}	Co^{III}/Co^{II}	Fe^{III}/Fe^{II}
ΔE	−0.61	−2.67	−1.07	0.94

The Cr^{III} dopant does not follow this trend, and its replacement energy is much higher than expected from its ionic radius, which can be attributed to the instability of Cr^{III} in tetrahedral coordination, as confirmed by the scarcity of inorganic complexes with tetrahedral Cr^{III}. The crystal field stabilization energy of octahedral and tetrahedral Cr^{III} has been estimated for oxides with the spinel structure.[40,41] The resulting values are 2.33 eV for octahedral Cr^{III} and 0.69 eV for tetrahedral Cr^{III}, with a difference of 1.64 eV. This value has the same order of magnitude as the energy difference of ∼1.20 eV required in our calculations for bringing the replacement energy ΔE_{III} of Cr^{III} in AlPO-34 in line with the trend observed for the other Me^{III} dopants.

Our calculations confirm the marked preference of Cr^{III} for octahedral coordination, and we expect the substitution of Cr^{III} in the tetrahedral sites of AlPOs to be unstable and difficult to achieve experimentally. Our finding is consistent with the experimental evidence, which supports the idea that Cr^{III} is not tetrahedrally coordinated in the AlPO framework but rather octahedrally coordinated with two extra water ligands, as originally suggested by Chen and Sheldon.[42]

3.4. Redox Properties. Combining the energetic information obtained for the Me^{III} dopants in this paper, and for the Me^{II} dopants in ref 5 we can evaluate the redox energy for the Me^{II}/Me^{III} couples in the MeAlPO catalysts. The energy is calculated according to eq 3, in which we use hydrogen as reductant

$$Me^{III}AlPO-34 + {}^1/_2H_2 \xrightarrow{\Delta E} Me^{II}\,HAlPO\text{-}34 \qquad (3)$$

The calculated redox potentials are summarized in Table 6 and clearly indicate that, among the transition metal ions investigated, Fe is most stable in the 3+ oxidation state, whereas Mn is the most stable as 2+ ion. Cr and Co, instead, have intermediate behavior and can switch more easily between the two oxidation states. We had previously examined the redox behavior of the Co^{II}/Co^{III} couple in AlPO-34 in a computational study that employed a different Hamiltonian (DFT-GGA, as opposed to the HF of the present work), code, and computational settings. It is reassuring to note that the calculated reaction energy for the Co^{II}/Co^{III} redox couple is consistent in the two cases: −1.18 eV in ref 11 and −1.07 eV here, which indicates the validity of the computational results obtained.

3.5. Catalytic Activity. When correlating the redox energies reported in Table 6 with the activity of different MeAlPO catalysts, we need to consider the mechanistic steps involved in the catalytic cycle. Results will in general differ for each reaction examined; however, the scale of redox strength proposed in Table 6, when coupled with experimental data on the catalytic activity of different Me^{III}/Me^{II} dopant ions in the same AlPO framework, can help us identify the mechanistic details of the catalytic reaction.

As a general rule, each redox catalytic process will involve at least two elementary steps, which we can identify with the reduction of the Me^{III} dopant to Me^{II} and with its reoxidation from the 2+ to the 3+ oxidation state. The relative performance of the different Me^{II}/Me^{III} dopants examined here will depend on which elementary step is rate determining for the catalytic reaction and on the experimental conditions examined. Of course, framework type, temperature, and partial pressures of reagents and products can each influence the relative rates of the two elementary steps involving the Me dopant, and hence also the relative activity of Fe, Co, Mn, and Cr−AlPO catalysts.

If we assume that the rate determinig step in the catalytic cycle involves the reduction of the Me^{III} to Me^{II} state, our calculations would predict the relative activity to decrease in the order of Mn−AlPO > Co−AlPO > Cr−AlPO > Fe−AlPO. If instead the rate determining step involves the reoxidation of the Me^{II} dopant ion to Me^{III}, we would expect a reverse order of activity, i.e., Fe−AlPO > Cr−AlPO > Co−AlPO > Mn−AlPO. Finally, if the two elementary steps described above have a comparable rate, we would expect Cr−AlPO and Co−AlPO catalysts to be the most active, as Cr and Co are the ions that can more easily change their oxidation state in either direction. This knowledge on the redox potential can be applied to investigate the experimental results of redox reactions catalyzed by MeAlPOs.

Thomas et al.[4] have reported that Fe−AlPOs show a remarkably high catalytic activity for the selective oxidation of cyclohexane in air (403 K and 15 bar of dry air); the results of the catalytic activity of Fe−AlPOs are superior to those of the Co and Mn-substituted analogues. The authors attributed this result to the fact that only a small proportion of Co^{II} and Mn^{II} ions that are isomorphously incorporated into the AlPO-36, AlPO-11, and AlPO-5 structures are convertible into the +3 oxidation state by O_2 or dry air,[30] in contrast to the situation with Fe^{II} and Fe^{III} states.[43] This behavior, which was not properly understood in the experimental work, is in agreement with our results: fewer Mn^{II} and Co^{II} ions can be oxidized by molecular oxygen because these ions are more stable than Fe in the +2 oxidation state. Oxidizing Mn^{II} and Co^{II} dopant ions in the AlPO framework is energetically unfavorable and will therefore be difficult to achieve, in particular for the Mn active center. Experimentally, the mechanism for the oxidation of cyclohexane was found to involve free radicals. In light of our results, we suggest that the rate-determining step for this catalytic reaction is the oxidation of the Me^{II} ions, whereas the reduction of Me^{III} by abstraction of an H radical from the reagent is faster and not rate-determining. MnAlPO and CoAlPO catalysts are less active for this reaction, as the oxidation of Mn^{II} and Co^{II} is energetically more difficult.

In the case when the rate-determining step consists of the reduction of the Me^{III} center, we expect Mn and Co doped materials to be the most active. An example of this situation has been reported by Thomas et al.[4] For the regioselective oxidation of linear alkanes by molecular oxygen, MnAlPO and CoAlPO are found to be superior to the inorganic catalysts which use sacrificial oxidants. In the course of the partial oxidation, the transition metal ions are reduced to their 2+ state. The above scale of catalytic activity suggests that the reduction of the active site metal dopant is the rate determining step for the oxidation of linear alkanes in the experimental conditions employed.

If the catalytic cycle involves a reduction of the Me^{III} and its subsequent reoxidation with a similar rate, the catalytic activity will be related to the ability of the metal ion to switch between its different oxidation states. In this case, Cr will have the highest catalytic activity as its Me^{II}/Me^{III} redox potential has the lowest absolute value in our scale of calculated redox energies (Table 6). Experimental results by Luna et al.,[8] concerning the study of the redox catalytic activity of different metal dopants in the AlPO−VFI framework, for the oxidation of cyclohexane under mild conditions, show that CrAPO has the highest activity and MnAPO the lowest.

Comparing the relative activity of different metal dopants in the oxidation of cyclohexane from the works of Thomas et al.[4] and Luna et al.[8] suggests that the cyclohexane oxidation proceeds via different mechanisms in small and large pore AlPO catalysts. The AlPO−VFI structure has a larger pore size than the AlPO-34 examined here and also of the catalysts used in the work of Thomas et al. In a small-pore material, the cyclohexane molecule can only penetrate with difficulty into the micropores of the catalysts and is always in close contact with the walls of the structure. Upon contact of the hydrocarbon with the Me^{III} active center, one of the terminal hydrogens is extracted to yield Me^{II} in the framework and an organic radical that will subsequently react with molecular oxygen. In the constrained environment of a small-pore catalyst, the contact between organic reagent and active site is much more effective than in a large pore material; this step will be fast (not rate-determining) in the former case, whereas in large-pore catalysts, it can differentiate the redox activity of the Me^{III} dopants. In the small pore catalysts, the rate determining step appears instead to be associated with the migration of the organic radical away from the active site, and the subsequent reoxidation of the Me^{II} ion with molecular oxygen. The catalytic activity in small-pore catalysts is differentiated by the latter step. The experimental results, coupled with our calculated redox energies, suggest that the reoxidation of the Me^{II} center is important also in the large pore VFI-type catalysts. The scale of the experimental activity is in fact consitent with a mechanism in which oxidation of Me^{II} and the hydrogen abstraction from the cyclohexane have comparable rate. The highest activity in the cyclohexane oxidation is therefore given by Fe (the easiest to oxidize to 3+) in small-pore catalysts, and by Cr (the easiest to switch between 2+ and 3+) in large-pore materials.

4. Conclusion

We have studied, using ab initio QM methods, the structure and redox properties of trivalent metal dopants in AlPO-34. From the results of our calculations and comparison with experiment, we conclude the following points:

(1) The local environment of trivalent Co and Mn dopants is a distorted tetrahedron due to Jahn−Teller distortions. Cr^{III}, Fe^{III}, and closed shell dopants have a more symmetric coordination.

(2) The deviation of the calculated T−O−P angles between the doped and the undoped AlPO structure provides a way of estimating the range of the structural distortion around the metal dopant. The structural strain caused by tri-valent dopants is short-ranged and does not propagate to undoped regions of the host AlPO framework.

(3) The nature of bonding between the Me^{III} dopants and the neighboring oxygens is ionic in nature; the ionicity of the Me−O bonds explains the Lewis acidity of the Me^{III} ions, which are able to increase their coordination number in the presence of Lewis bases.

(4) The replacement energy ΔE_{III} of the 3+ dopant ions in AlPO-34 increases linearly as a function of the Me-O bond distance: the larger the size of the metal dopant, the more difficult its inclusion in the AlPO framework. Cr^{III} is unstable in tetrahedral sites, because of crystal field effects, and therefore, inclusion of Cr^{III} in the AlPO framework will be difficult to achieve experimentally.

(5) The calculated redox energies of the Me^{II}/Me^{III} couples indicate that, among the transition metal ions investigated, Fe is the most stable in the 3+ oxidation state, whereas Mn is the most stable as 2+ ion. Cr and Co, instead, have intermediate behavior and can switch more easily between the two oxidation states. These results contribute to elucidate the mechanistic details of catalytic processes occurring in MeAlPOs.

Acknowledgment. We are grateful to Dr. G. Sankar for useful discussions. We would like to thank EPSRC for funding this research via a studentship to I.S. and an Advanced Research Fellowship to F.C. The Royal Society is gratefully acknowledged for funding the computational resources employed.

References and Notes

(1) Thomas, J. M.; Thomas, W. J. *Principles and Practice of Heterogeneous Catalysis*; VCH: Weinheim, Germany, 1996.
(2) Corma, A. *Catal. Today* **1997**, *38*, 257.
(3) Sheldon, R. A.; Kochi, J. K. *Metal catalyzed Oxidations of Organic compounds*; Academic Press: New York, 1981.
(4) Thomas, J. M. *Angew. Chem. Int. Ed. Engl.* **1994**, *33*, 913.
(5) Saadoune, I.; Corà, F.; Catlow, C. R. A. *J. Phys. Chem.* **2003**, *107*, 3003.
(6) Thomas, J. M.; Raja, R.; Sankar, G.; Bell, G. R. *Nature* **1999**, *398*, 227.
(7) Schuchardt, U.; Carvalho, W. A.; Spinacé, E. V. *Synlett*. **1993**, *10*, 713.
(8) Luna, F. J.; Ukawa, S. E.; Wallau, M.; Schuchardt, U. *J. Mol. Catal. A: Chem.* **1997**, *117*, 405.
(9) Saunders, V. R.; Dovesi, R.; Roetti, C.; Causà, M.; Harrison, N. M.; Orlando, R.; Zicovich-Wilson, M. C.; Doll, K.; Civalleri, B. *CRYSTAL 2001 User's Manual*; University of Torino: Turin, Italy, 2001.
(10) www.chimifm.unito.it/teorica/crystal/Basis_Sets/mendel.html.
(11) Corà, F.; Catlow, C. R. A.; D'Ercole, A. *J. Mol. Catal. A* **2001**, *166*, 87.
(12) Sankar, G.; Thomas, J. M. *Top. Catal*. **1999**, *8*, 1.
(13) Sankar, G.; Thomas, J. M.; Catlow, C. R. A. *Top. Catal*. **2000**, *10*, 225.
(14) Lok, B. M.; Messina, C. A.; Patton, R. L.; Gajek, R. T.; Cannan, T. R.; Flanigen, E. M. *J. Am. Chem. Soc*. **1984**, *106*, 6092.
(15) Chen, J. S.; Thomas, J. M.; Sankar, G. *J. Chem. Soc., Faraday Trans.* **1994**, *90*, 3455.
(16) (a)Hehre, W. J.; Ditchfield, R.; Pople, J. A. *J. Chem. Phys.* **1972**, *56*, 2257, b) Hariharan, P. C.; Pople, J. A. *Theor. Chim. Acta*. **1973**, *28*, 213.
(17) Kirishnan, R.; Binkley, J. S.; Seeger, R.; Pople, J. A. *J. Chem. Phys.* **1980**, *72*, 650.
(18) Frisch, M. J.; Trucks, G. W.; Schlegel, H. B.; Scuseria, G. E.; Robb, M. A.; Cheeseman, J. R.; Zakrzewski, V. G.; Montgomery, J. A., Jr.; Stratmann, R. E.; Burant, J. C.; Dapprich, S.; Millam, J. M.; Daniels, A. D.; Kudin, K. N.; Strain, M. C.; Farkas, O.; Tomasi, J.; Barone, V.; Cossi, M.; Cammi, R.; Mennucci, B.; Pomelli, C.; Adamo, C.; Clifford, S.; Ochterski, J.; Petersson, G. A.; Ayala, P. Y.; Cui, Q.; Morokuma, K.; Malick, D. K.; Rabuck, A. D.; Raghavachari, K.; Foresman, J. B.; Cioslowski, J.; Ortiz, J. V.; Stefanov, B. B.; Liu, G.; Liashenko, A.; Piskorz, P.; Komaromi, I.; Gomperts, R.; Martin, R. L.; Fox, D. J.; Keith, T.; Al-Laham, M. A.; Peng, C. Y.; Nanayakkara, A.; Gonzalez, C.; Challacombe, M.; Gill, P. M. W.; Johnson, B. G.; Chen, W.; Wong, M. W.; Andres, J. L.; Head-Gordon, M.; Replogle, E. S.; Pople, J. A. *Gaussian 98*, revision A.6; Gaussian, Inc.: Pittsburgh, PA, 1998.
(19) Rudolph, W. W.; Manson, R.; Pye, C. C. *Phys. Chem. Chem. Phys.* **2000**, *2*, 5030.
(20) Rudolph, W. W.; Pye, C. C.; Lrmer, G. *J. Raman Spectosc*. **2002**, *33*, 177.
(21) Akesson, R.; Pettersson, L. G. M.; Sandstrom, M.; Wahlgren, U. *J. Am. Chem. Soc*. **1994**, *116*, 8691.
(22) Bol, W.; Welzen, T. *Chem. Phys. Lett*. **1977**, *49*, 189.
(23) Muñoz-Páez, A.; Diaz-Moreno, S.; Marcos, E. S.; Martinez, J. M.; Pappalardo, R. R.; Persson, I.; Sandström, M.; Pattanaik, S.; Lindqvist-Reis, P. *J. Phys. IV* **1997**, *7*, C2−647.
(24) Beattie, J. K.; Best, S. P.; Skelton, B. W.; White, A. H. *J. Chem. Soc., Dalton Trans.* **1981**, *10*, 2105.
(25) Herdman, G. J.; Neilson, G. W. *J. Phys. Condens. Matter*. **1992**, *4*, 649.
(26) Wolfram, W. R.; Roger, M.; Cory, C. P. *Phys. Chem. Chem. Phys*. **2000**, *2*, 5030.
(27) Shannon, R. D.; Prewitt, C. T. *Acta Cryst.* **1970**, *B26*, 1046.
(28) Corà, F.; Sankar, G.; Catlow, C. R. A.; Thomas, J. M. *Chem. Commun*. **2002**, 734.
(29) Zenonos, C.; Sankar, G.; Corà, F.; Lewis, D. W.; Pankhurst, Q. A.; Catlow, C. R. A.; Thomas, J. M. *Phys. Chem. Chem. Phys*. **2002**, *4*, 5421.

(30) Barrett, P. A.; Sankar, G.; Catlow, C. R. A.; Thomas, J. M. *J. Phys. Chem*. **1996**, *100*, 8977.
(31) Thong, N.; Schwarzenbach, D. *Acta Cryst. A* **1979**, *35*, 658.
(32) Goiffon, A.; Bayle, G.; Astier, R.; Jumas, J. C.; Maurin, M.; Philippot, E. *Rev. Chem. Miner*. **1983**, *20*, 338.
(33) Corà, F.; Catlow, C. R. A.; Civalleri, B.; Orlando, R. In preparation.
(34) Sankar, G.; Thomas, J. M.; Catlow, C. R. A. *Top. Catal*. **2000**, *10*, 255.
(35) Tuel, A.; Caldarelli, S.; Meden, A.; McCusker, L. B.; Baerlocher, C.; Ristic, A.; Rajic, N.; Mali, G.; Kaucic, V. *J. Phys. Chem. B* **2000**, *104*, 5697.
(36) Peeters, M. P. J.; van de Ven, L. J. M.; de Haan, J. W.; van Hooff, J. H. C. *J. Phys. Chem*. **1993**, *97*, 8254.
(37) Jänchen, J.; Peeters, M. P. J.; van Wolput, J. H. M. C.; Wolthuizen, J. P.; van Hooff, J. H. C. *J. Chem. Soc., Faraday Trans*. **1994**, *90*, 1033.
(38) Corà, F.; Saadoune, I.; Catlow, C. R. A. *Angew. Chem. Int. Ed.* **2002**, *114*, 4677.
(39) Corà, F. Unpublished results.
(40) Escalante, D.; Giraldo, L.; Pinto, M.; Pfaff, C.; Sazo, V.; Mat-Jushin, M.; Méndez, B.; López, C. M.; Machado, F. J.; Gold-wasser, J.; Ramírez de Agudelo, M. M. *J. Catal*. **1997**, *169*, 176.
(41) West, A. R. *Basic Solid State Chemistry*; Wiley: Chichester, U.K., 1988.
(42) Chen, J. D.; Sheldon, R. A. *J. Catal*. **1995**, *153*, 1.
(43) Raja, R.; Sankar, G.; Thomas, J. M. *J. Am. Chem. Soc*. **1999**, *121*, 11926.